Report

Cell Reports

Lhx2 Expression in Postmitotic Cortical Neurons Initiates Assembly of the Thalamocortical Somatosensory Circuit

Graphical Abstract

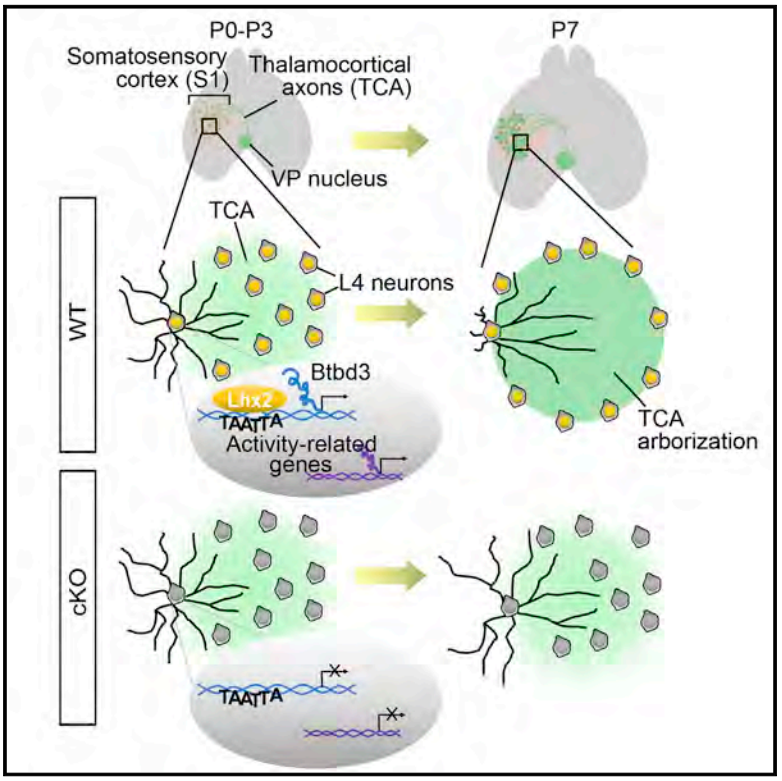

Authors

Chia-Fang Wang, Hsiang-Wei Hsing, Zi-Hui Zhuang, ..., Marta Nieto, Bai Chuang Shyu, Shen-Ju Chou

Correspondence

schou@gate.sinica.edu.tw

In Brief

Wang et al. find that the transcription factor Lhx2 functions in postmitotic cortical neurons to initiate barrel cortex formation. Lhx2 induces the expression of activity-regulated genes that enable layer 4 neurons in the somatosensory cortex to respond to thalamocortical inputs, develop dendritic asymmetry, and form cellular barrels.

Highlights

- Lhx2 in postmitotic cortical neurons is critical for barrel cortex development
- Deletion of Lhx2 in postmitotic neurons leads to somatosensory functional deficits
- The expression of activity-regulated genes during S1 development requires Lhx2
- Lhx2 directly induces Btbd3 to regulate layer 4 neuron dendritic development

Accession Numbers

GSE92372

Wang et al., 2017, Cell Reports *18*, 849–856
January 24, 2017
http://dx.doi.org/10.1016/j.celrep.2017.01.001

Cell Reports
Report

Lhx2 Expression in Postmitotic Cortical Neurons Initiates Assembly of the Thalamocortical Somatosensory Circuit

Chia-Fang Wang,[1] Hsiang-Wei Hsing,[1] Zi-Hui Zhuang,[1] Meng-Hsuan Wen,[1] Wei-Jen Chang,[2] Carlos G. Briz,[3] Marta Nieto,[3] Bai Chuang Shyu,[2] and Shen-Ju Chou[1,4,*]
[1]Institute of Cellular and Organismic Biology, Academia Sinica, Taipei 11529, Taiwan
[2]Institute of Biomedical Sciences, Academia Sinica, Taipei 11529, Taiwan
[3]Centro Nacional de Biotecnología, CNB-CSIC, Darwin 3, Campus de Cantoblanco, Madrid 28049, Spain
[4]Lead Contact
*Correspondence: schou@gate.sinica.edu.tw
http://dx.doi.org/10.1016/j.celrep.2017.01.001

SUMMARY

Cortical neurons must be specified and make the correct connections during development. Here, we examine a mechanism initiating neuronal circuit formation in the barrel cortex, a circuit comprising thalamocortical axons (TCAs) and layer 4 (L4) neurons. When *Lhx2* is selectively deleted in postmitotic cortical neurons using conditional knockout (cKO) mice, L4 neurons in the barrel cortex are initially specified but fail to form cellular barrels or develop polarized dendrites. In *Lhx2* cKO mice, TCAs from the thalamic ventral posterior nucleus reach the barrel cortex but fail to further arborize to form barrels. Several activity-regulated genes and genes involved in regulating barrel formation are downregulated in the *Lhx2* cKO somatosensory cortex. Among them, *Btbd3*, an activity-regulated gene controlling dendritic development, is a direct downstream target of Lhx2. We find that Lhx2 confers neuronal competency for activity-dependent dendritic development in L4 neurons by inducing the expression of Btbd3.

INTRODUCTION

The barrel cortex, a major part of the primary somatosensory cortex (S1), receives and processes inputs from major facial whiskers in a topographic fashion. The barrels are located in cortical layer 4 (L4) and consist of L4 spiny stellate neurons forming cell-dense rings or "cellular barrels" and thalamocortical axons (TCAs) that occupy the barrel hollow. L4 neurons develop polarity and extend dendrites asymmetrically to the hollow upon receiving TCA inputs in the first postnatal week (Erzurumlu and Gaspar, 2012; Li and Crair, 2011; Wu et al., 2011). Assembly of the barrel cortex circuit is critical for somatosensation in rodents, and it requires finely tuned coordination between cortical and thalamic neurons.

Previous studies of genetically modified mice demonstrated that the establishment of neuronal connections and the transmission of neuronal activity from whiskers to the L4 neurons in S1 are required for barrel formation. Deletion of factors functioning in glutamatergic or serotonergic neurotransmission perturbs the formation of patterned TCA inputs and/or the aggregation of L4 neurons (Erzurumlu and Gaspar, 2012; Li and Crair, 2011; Vitali and Jabaudon, 2014; Wu et al., 2011). Furthermore, several activity-dependent transcription factors, such as Lmo4, NeuroD2, and Btbd3, were reportedly involved in the formation of cellular barrels or the development of polarized dendritic patterns (Ince-Dunn et al., 2006; Kashani et al., 2006; Matsui et al., 2013). In spite of these studies, the molecular mechanisms initiating barrel cortex development remain largely unknown. For example, it remains to be determined how L4 neurons acquire the capacity to respond to TCA inputs, and reciprocally, how cortical neurons instruct thalamic axons during barrel cortex formation.

Lhx2, a LIM homeodomain transcription factor that functions to specify multiple cell types (Shirasaki and Pfaff, 2002), is highly expressed in cortical neurons located in the superficial layers embryonically and in the first postnatal weeks (Bulchand et al., 2003; Nakagawa et al., 1999). A previous report showed that conditional *Lhx2* deletion in cortical progenitors using a late-onset *Emx1*-Cre perturbs barrel formation (Shetty et al., 2013), implying that cortical expression of Lhx2 regulates barrel cortex development. However, dramatic defects in neurogenesis, cortical layer formation, and cortical patterning were reported when Lhx2 was deleted in the cortical progenitors (Chou and O'Leary, 2013; Chou et al., 2009; Hsu et al., 2015; Shetty et al., 2013), making it difficult to delineate the postmitotic function of Lhx2 in barrel development. Here, by deleting *Lhx2* specifically in postmitotic cortical neurons with *Nex*-Cre (Goebbels et al., 2006), we find that Lhx2 is required for L4 neurons to form cellular barrels and for the TCAs to extensively arborize in the barrel cortex. Further, Lhx2 induces the expression of several activity-regulated genes and enables cortical neurons to respond to TCA inputs. These findings indicate that Lhx2 acts as a molecular switch in cortical neurons to initiate somatosensory circuit assembly.

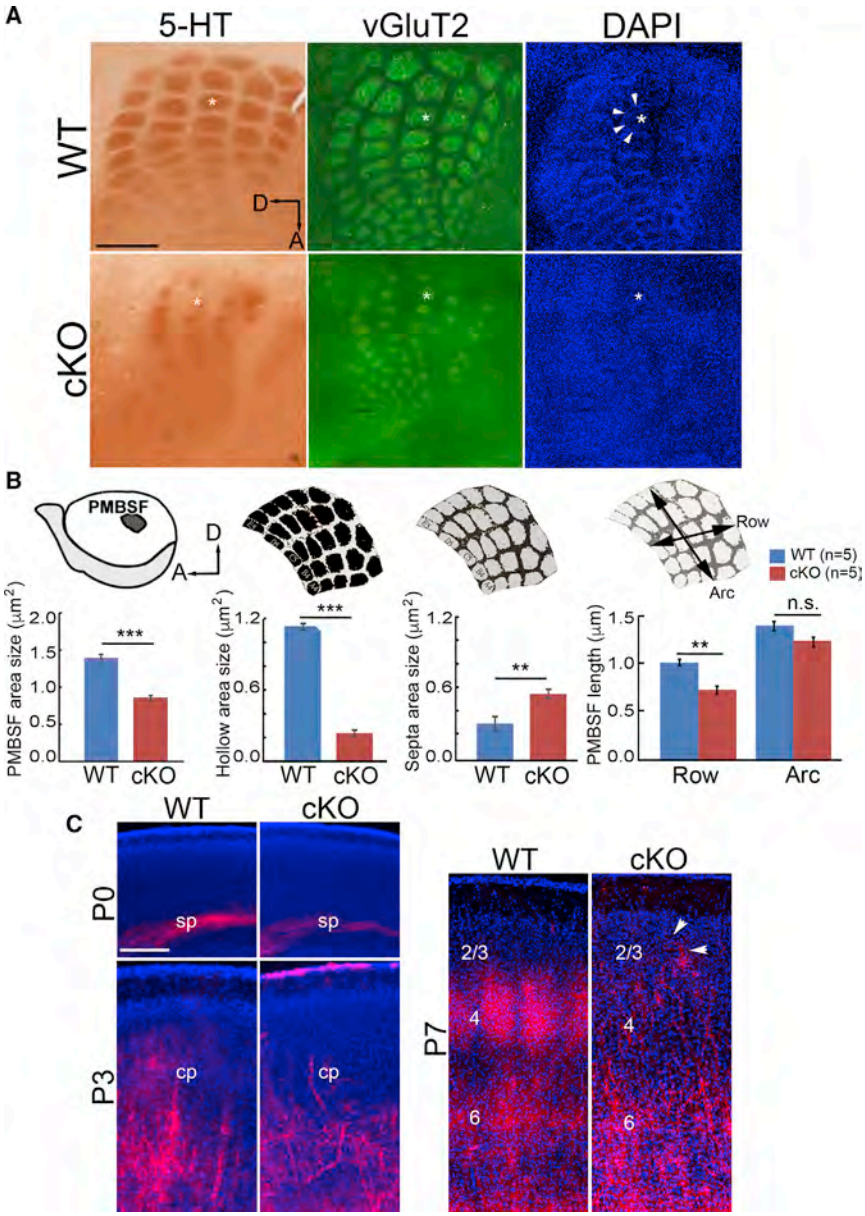

Figure 1. *Lhx2* cKO Mice Show Defects in Barrel Formation

(A) Immunostaining for 5HT and vGluT2 and DAPI nuclear staining on tangential sections of flattened cortex of WT (wild-type) and cKO ($Lhx2^{f/f}$;*Nex*-Cre) mice at P7. The 5HT- and vGluT2-positive TCA inputs filled the barrel hollow (for example, C2, marked with an asterisk [*]). Cellular barrels (arrowheads) were apparent in WT but were not detected in the cKO samples. D, dorsal; A, anterior.

(B) Comparison of WT and cKO S1. The size of PMBSF was significantly decreased in cKO S1 ($p < 0.001$), with decreased area size of hollow ($p < 0.001$) and increased area size of septa ($p < 0.01$). The length of PMBSF along rows was decreased ($p < 0.01$), while no significant difference was found in the length of PMBSF along the arc (n.s., not significant, $p > 0.05$).

(C) TCA projections are labeled by DiI (red) injected into VP of the thalamus in WT and cKO brains. Coronal sections were counterstained with DAPI. In WT and cKO mice, VP neuronal axons can reach the subplate (sp) and cortical plate (cp) in S1 at P0 and P3, respectively. At P7, while VP TCAs in WT arborize in layer 4 (4) to fill the barrel hollow, VP TCAs in cKO mice fail to arborize in L4, and some axonal terminals (arrowheads) remain in layers 2/3 (2/3). Scale bars, 200 μm. See also Figures S1 and S2.

RESULTS

The Absence of Lhx2 in Postmitotic Neurons Leads to Anatomical Defects in Barrel Cortex Development

Lhx2 is highly expressed in neurons located in layers 2/3 (L2/3) and L4 (Bulchand et al., 2003; Nakagawa et al., 1999), but its precise functions in these postmitotic neurons have not been fully addressed. In mice, once cellular barrels become apparent at postnatal day 7 (P7), Lhx2 expression in L4 of the somatosensory cortex becomes more concentrated in the barrel wall (Figure S1A), suggesting that it functions in L4 neurons regulating barrel formation. We thus investigated barrel cortex development in the *Lhx2* cKO ($Lhx2^{f/f}$; *Nex*-Cre) brains, where *Lhx2* is selectively deleted in postmitotic neurons by *Nex*-Cre (Goebbels et al., 2006).

The location of TCAs targeting the primary sensory areas was determined by immunostaining with antibodies against 5HT and vGluT2 on tangential sections of flattened cortices (Figures 1A and S1B). In contrast to the nearly complete loss of TCA inputs in the cortices where *Lhx2* was deleted by late-onset *Emx1*-Cre (Shetty et al., 2013), the conditional knockout (cKO) mice had detectable 5HT- and vGluT2-positive primary sensory areas, including S1, A1 (primary auditory area), and V1 (primary visual area) (Figure S1B; Zembrzycki et al., 2015). Among the primary sensory areas, the size of S1 in cKO mice was the most dramatically diminished. This change was not due to changes in cortical size, as no major differences were found in the cortical size between cKO and wild-type (WT) mice (including $Lhx2^{f/f}$, $Lhx2^{f/+}$, $Lhx2^{f/+}$;*Nex*-Cre, and $Lhx2^{+/+}$;*Nex*-Cre) (Figure S1C; Chou et al., 2009; Zembrzycki et al., 2015). We found that the size of the posterior medial barrel subfield (PMBSF), the major component of the S1, was significantly decreased in cKO mice (Figures 1A and 1B). Within the cKO PMBSF, barrels were disproportionally decreased in size: the area of the vGluT2-positive hollow was significantly decreased, and the vGluT2-negative septal area was significantly increased (Figure 1B). Further, we observed enlarged spacing between barrel rows in cKO PMBSF, where adjacent barrels in two rows were further apart than adjacent barrels within the same row (Figure 1A). This led to significantly decreased length of PMBSF along rows, while the length

along arc remained similar in cKO and WT mice (Figure 1B). This result suggests that Lhx2 in the postmitotic neurons patterns the distribution of TCAs in S1.

To further examine the development of TCAs in cKO mice, we inserted DiI (1,1-dioctadecyl-3,3,3',3'-tetramethyl-indocarbocyanine perchlorate) crystals into the thalamic ventral posterior nucleus (VP) to track VP axonal projections at various time points in the first postnatal week. In both WT and cKO brains, VP TCAs reached the subplate underneath S1 at P0 and extended to superficial layers in the cortical plate at P3 (Figure 1C). At P7, however, while VP TCAs arborized extensively in WT L4 to occupy barrel hollows, they were more sparsely branched in cKO L4 with an increase of branches and terminal endings in L2/3 (Figures 1C and S1D). Thus, *Lhx2* deletion in postmitotic cortical neurons did not impede VP TCAs entering S1; instead, it led to their arborization defects.

We then asked whether the cKO L4 neurons form cellular barrels, the cell-dense rings enclosing TCA patches. We observed cellular barrels by P7 in WT mice, but not in cKO mice (Figure 1A). We measured the cell density across the C2 barrel by DAPI staining on tangential sections of P7 WT and cKO cortices (Figure S1E). We observed higher L4 cell density in septa (with weaker vGluT2 staining) than in hollows (with stronger vGluT2 staining) in WT mice, while L4 cells distributed evenly across barrels in cKO mice (Figures S1F and S1G). Further, we found cellular barrels remained undetectable at P20 (Figure S1H), confirming that barrel formation was not simply delayed in cKO mice. Thus, we concluded that the loss of Lhx2 in postmitotic neurons leads to defects in cellular barrel formation.

To verify that the loss of cellular barrels in cKO mice was not due to the failure of L4 neurons to migrate to their correct layer, we first examined the migration of L4 neurons in WT and cKO brains. We found in both WT and cKO brains, most of the neurons generated on embryonic day 14.5 (E14.5) located in L4 at P7 (Figure S2A). Further, we performed in utero electroporation at E14.5 to deliver CAG-Cre and CAG-mCherry plasmids into L4 neurons in *Lhx2*$^{f/+}$ and *Lhx2*$^{f/-}$ cortices. In this system, the expression of Cre recombinase generates WT (*Lhx2* heterozygous) and *Lhx2* mutant cells in *Lhx2*$^{f/+}$ and *Lhx2*$^{f/-}$ cortices, respectively, and mCherry expression labels transfected cells. We confirmed the absence of Lhx2 expression in the transfected cells in *Lhx2*$^{f/-}$ cortices (Figure S2B) and that the majority of mCherry-expressing cells are located in L4 in both *Lhx2*$^{f/+}$ and *Lhx2*$^{f/-}$ cortices at P7 (Figures S2C and S2D), indicating that *Lhx2* loss did not lead to L4 neuron migration defects.

Barrel Cortex Showed Functional Deficits in *Lhx2* cKO Mice

As proper connection from whiskers to S1 is required for cellular barrel formation (Ding et al., 2003; Erzurumlu and Kind, 2001; Rebsam et al., 2005), we used CO (cytochrome oxidase) staining to examine the somatosensory pathway in the cKO mice. We observed no detectable difference in size or organization of barreloids and barrelettes, respective somatosensory nuclei in the dorsal thalamus and brainstem, between *Lhx2* cKO and WT brains (Figure S2E). Thus, the anatomical defects we observed in cKO brains were the result of the defective cortical or thalamocortical somatosensory circuit.

Previous studies suggested that defective barrel cortex development is associated with aberrant sensory responsiveness (Petersen, 2007). To test the selective functionality of barrels, we shaved all but the C2 whisker on one side of the head and let the mice explore an enriched environment for 1 hr. We then analyzed the distribution of c-Fos-positive neurons (i.e., the activated neurons) in S1 L4. Although most c-Fos-positive cells were concentrated at the location of the C2 barrel in both WT and cKO mice (Figure 2A), we found a higher proportion of c-Fos-positive neurons located outside the C2 barrel in cKO mice when compared with WT littermates (Figure 2B). This suggested that the cKO S1 failed to receive precisely mapped activity from the whiskers.

We further assessed the function of the whisker-to-S1 pathway in cKO mice with a multichannel probe at S1 to record field potential in multiple cortical layers simultaneously upon whisker stimulations. We compared the current source densities (CSDs) evoked by whisker electric stimulation in WT and cKO mice (Chen et al., 2008; Yang et al., 2006). The CSD profiles across the depth of S1 following whisker stimulation showed that sink currents were first detected in the L4 in both WT and cKO mice (Figures 2C and 2D). However, significantly decreased amplitude and increased latency of the whisker-evoked prominent sink currents in L4 were found in cKO mice than in WT mice (Figure 2E). This demonstrated that cKO shows functional deficits in responding to whisker sensory stimuli. Thus, we concluded that in cortical neurons, Lhx2 plays critical roles assembling the functional somatosensory circuitry.

Lhx2 Regulates Crucial Genetic Pathways in L4 Neurons to Enable Barrel Formation

We next investigated the molecular mechanisms underlying Lhx2 regulation of barrel formation. We performed microarray analyses with RNA collected from P7 WT and cKO S1. We found 2,765 transcripts showing altered expression levels in WT and cKO mice (unpaired t test, $p < 0.05$, $n = 3$), with 1,416 upregulated and 1,349 downregulated. Among them, 2,069 genes were annotated, and 314 of them were shown to be involved in the nervous system development (GO: 0007399) by PANTHER gene ontology (GO) analysis (Mi et al., 2013). Within this category, the top GO terms were pallium development (GO: 0021543), telencephalon development (GO: 0021537), and regulation of dendritic development (GO: 0050773).

Interestingly, among the genes showed changed expression levels in cKO S1, many of them were reportedly regulated by neuronal activity (as shown in Table S1; Pouchelon et al., 2014; Rodríguez-Tornos et al., 2013). For example, we found that *RORb* expression was significantly downregulated in cKO mice at P7 (Figures S2F and S2G). The expression of *RORb* increases in the S1 L4 during barrel cortex development and decreases when TCA inputs are eliminated (Jabaudon et al., 2012; Pouchelon et al., 2014). Using in situ hybridization and qRT-PCR, we found the *RORb* expression level was comparable in WT and cKO mice at P0 (Figures S2F and S2G), suggesting that L4 neurons were initially specified in cKO mice. However, without Lhx2, *RORb* could not be fully induced in cKO S1 at P7.

The misregulation of these activity-regulated genes in cKO was likely associated with barrel formation defects. Thus, we

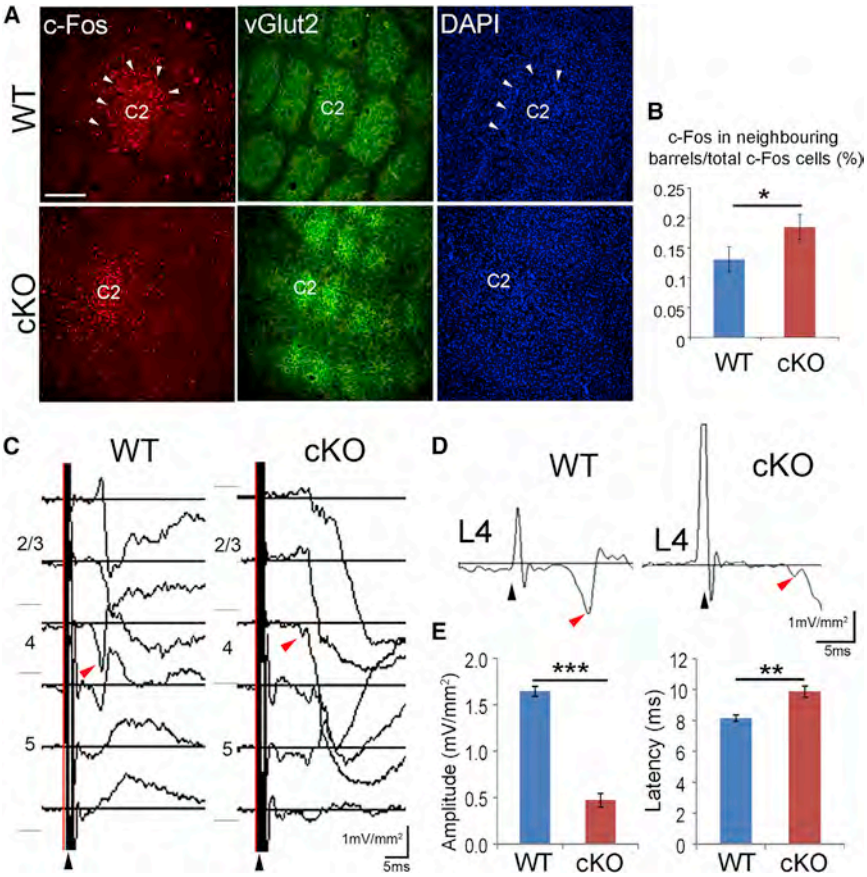

Figure 2. *Lhx2* cKO Mice Show Functional Deficits in Somatosensory Cortex

(A) Immunostaining for c-Fos and vGluT2 on tangential sections of flatten cortices from mice with only C2 whisker. DAPI counterstaining indicates barrel wall (arrowheads) are present in WT cortices, but not in cKO cortices. In both WT and cKO mice, the majority of c-Fos-positive cells are located in the C2 barrel.

(B) More c-Fos-positive neurons were located outside of the C2 barrel in cKO mice when compared with WT ($p < 0.05$, $n = 3$).

(C) Current source density (CSD) sweeps across the cortical layers in WT (left) and cKO (right) S1 upon electrical whisker stimulation. Black and red arrowheads indicate the stimulation and the first follow-up sink current response in layer 4, respectively.

(D) Cortical layer 4 (L4) sink current response in WT (left) and cKO (right) mice.

(E) The amplitude of the L4 sink current response was significantly decreased ($p < 0.001$, $n = 3$) and the latency was significantly higher ($p < 0.01$, $n = 3$) in cKO mice than in their WT littermates.

Scale bar, 100 μm. See also Figure S2.

compared the expression levels of genes reportedly regulating barrel formation in WT and cKO S1. We found that *Adcy1*, *Btbd3*, *Efna5*, and *Lmo4* were significantly downregulated in cKO S1 (Table S2; reviewed by Wu et al., 2011). qRT-PCR confirmed the downregulation of *Lhx2*, as well as *Adcy1*, *Btbd3*, *Efna5*, and *Lmo4* in cKO samples (Figure 3A). We also extended this analysis to confirm that the deletion of *Lhx2* in postmitotic neurons did not affect the expression of other genes involved in barrel development, including *mGluR5*, *NR1*, and *NeuroD2* (Figure S3A). These experiments suggest that Lhx2 regulates a specific set of key factors for barrel formation.

Lhx2 Is Required for Btbd3 Expression in the S1 through Direct Transcriptional Regulation

We then analyzed whether Lhx2 can directly regulate the expression of *Efna5*, *Adcy1*, *Lmo4*, and *Btbd3* genes. We identified multiple consensus Lhx2 binding sites (TAATTA, as described in Roberson et al., 1994) within 1 kb of the *Btbd3* upstream regulatory sequences and in the 4-kb upstream regulatory sequences of the *Efna5*, *Adcy1*, and *Lmo4* genes (Figures 3B and S3B). We tested the ability of Lhx2 to bind to these predicted sites by chromatin immunoprecipitation (ChIP) and found that in the P7 S1, Lhx2 showed significant binding to the most proximal Lhx2 binding site (BS3) in the *Btbd3* promoter region (Figure 3B), but not to the putative binding sites in the *Adcy1*, *Efna5*, or *Lmo4* promoter regions we tested (Figures S3B and S3C). As a control, we confirmed that in S1 at P7, Lhx2 does not bind to the *Pax6* enhancer (Hou et al., 2013), and this agrees with the fact that *Pax6* is not expressed in most postmitotic cortical neurons (Figures S3B and S3C). Without excluding the possibility for Lhx2 to regulate other genes directly through additional binding sites, here we focused on Lhx2 regulation of *Btbd3*. To confirm direct regulation of *Btbd3* by Lhx2, we showed that Lhx2 induced *Btbd3* promoter activity ~3-fold in N2a cells through the most proximal Lhx2 binding site (BS3). When this site is mutated (in m3, m13, m23, and m123), Lhx2 can no longer induce *Btbd3* promoter activity (Figure 3C). We next performed in situ hybridization to determine the expression pattern of *Btbd3* in P7 WT and cKO cortices. Utilizing *RORb* expression to mark L4 in WT and cKO S1, we found *Btbd3* was expressed in the WT S1 L4 at P7 but was not detectable in cKO S1 (Figure 3D), suggesting that Lhx2 is required for *Btbd3* expression in S1.

Lhx2 Regulation of Btbd3 Is Required for Proper Development of L4 Neuronal Dendritic Morphology

To confirm that Lhx2 is an upstream regulator for *Btbd3*, we next examined if the deletion of *Lhx2* in L4 neurons leads to defects in L4 neuronal dendritic polarity, similar to the result of knocking down *Btbd3* (Matsui et al., 2013). To target L4 neurons, we electroporated CAG-mCherry, CAG-Cre, and US2-LNL-GFP plasmids into $Lhx2^{f/+}$ and $Lhx2^{f/-}$ dorsal telencephalon at E14.5. CAG-Cre was electroporated at a low level to sparsely label cells. We used US2-LNL-GFP as a reporter, as Cre expression removes the neomycin gene and stop cassette between two *loxP* sites and allows GFP expression. We selected those neurons with cell bodies located on barrel walls and examined

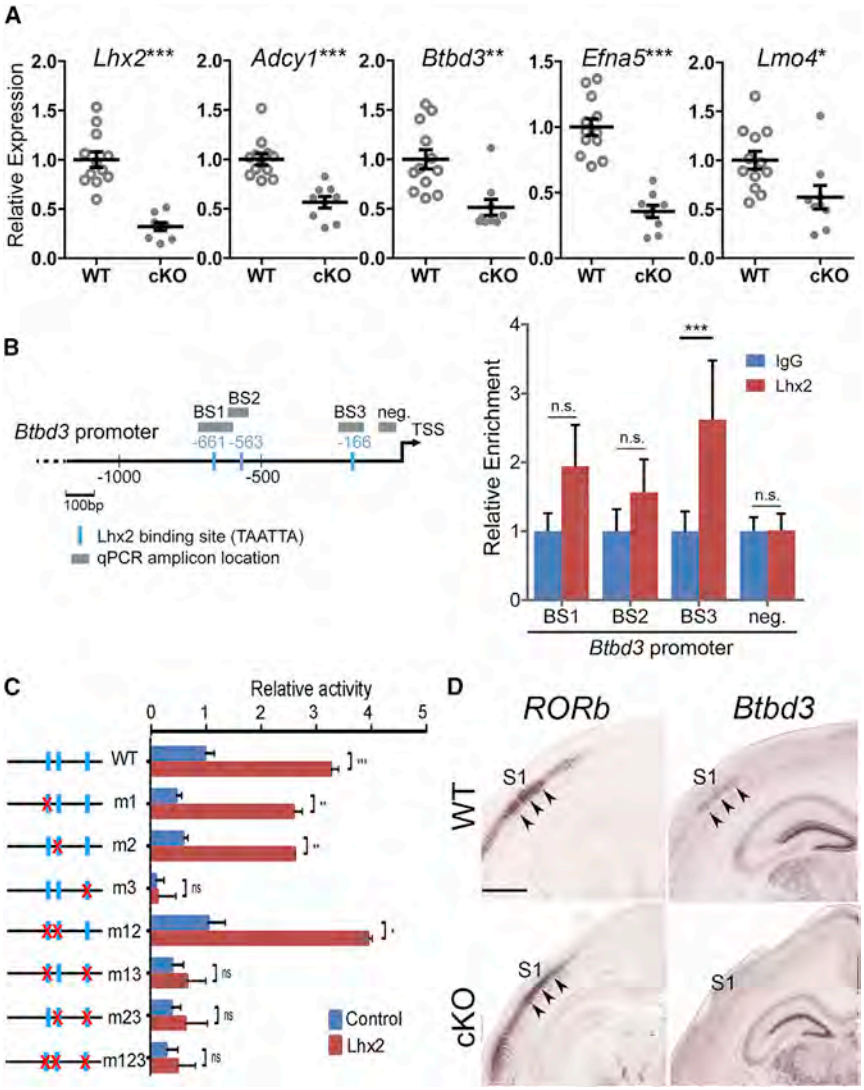

Figure 3. Lhx2 Regulates the Expression of Genes Functioning in Barrel Formation

(A) qRT-PCR analyses performed with RNA collected from S1 of WT and cKO cortices at P7. *Lhx2*, *Adcy1*, *Btbd3*, *Efna5*, and *Lmo4* expression was significantly decreased in cKO samples. Each dot represents one individual sample.

(B) Three consensus Lhx2 binding sites (BS1–3, blue boxes) were identified in the 1.3-kb *Btbd3* promoter. With ChIP analysis, anti-Lhx2 antibody showed a 2.6-fold enriched binding to BS3 when compared with IgG control ($p < 0.001$, $n = 8$).

(C) Lhx2 significantly increases *Btbd3* promoter activity ($p < 0.001$, $n = 4$) in N2a cells. The induction of *Btbd3* promoter activity by Lhx2 is lost only when the proximal Lhx2 binding site (BS3) is mutated.

(D) In situ hybridization for *RORb* and *Btbd3* on coronal sections of P7 WT and cKO cortices. *RORb* expression marks L4 in S1 (arrowheads) in both WT and cKO. *Btbd3* expression is detectable in WT S1 L4 (arrowheads), but not in cKO samples. Scale bar, 200 μm. See also Figures S3 and S4.

their dendritic morphology on tangential sections of flattened cortices. We found total dendritic length was similar in WT and mutant cells (Figures 4A and 4B). However, most dendrites of WT L4 cells projected to the hollow, the barrel center (Figures 4A and 4C), while the mutant cells showed significantly increased dendritic projections toward the septa and significantly decreased projections toward the hollow (Figures 4A and 4C). We further compared the polarity of WT and mutant cells with orientation bias index (OBI), which is the ratio of the length of hollow-projecting dendrites to the total dendrite length. The OBI of WT L4 neurons was close to 1, reflecting the fact that WT neurons are polarized, with most of their dendrites extending toward the hollow. Mutant L4 cells showed a significantly decreased OBI value (Figure 4D). As VP neurons in the thalamus were not affected in either $Lhx2^{f/+}$ or $Lhx2^{f/-}$ electroporated brains, our result indicated that *Lhx2* is required cell autonomously for the development of dendritic asymmetry in S1 L4 neurons.

We next asked whether Btbd3 expression was sufficient to rescue dendritic defects seen in *Lhx2* mutant L4 neurons. We generated a US-myc-Btbd3 expression construct and confirmed it directed Btbd3 overexpression when transfected in cell lines and in electroporated brains (Figures S4A–S4B′). Using a strategy similar to that described above, we electroporated CAG-mCherry, CAG-Cre, US2-LNL-GFP, and US2-myc-Btbd3 and found that total dendritic length was similar in WT and *Lhx2* mutant cells (Figures 4E and 4F). Btbd3 overexpression did not alter dendritic polarity in WT cells but re-established dendritic asymmetry in mutant cells (compare Figures 4E and 4G with Figures 4A and 4C). The OBI value was similar in *Btbd3* expressing WT and mutant cells (Figure 4H), indicating that lack of dendritic asymmetry in *Lhx2* mutant cells was mainly due to the lack of *Btbd3* expression. Taken together, we concluded that Lhx2 regulates the S1 L4 neuronal polarity by inducing *Btbd3* expression.

Lhx2 Regulates the Function of Btbd3 prior to the Activity-Regulated Events of Barrel Development

To further place the *Lhx2-Btbd3* genetic pathway in barrel cortex development, we examined the expression of *Btbd3* in several mutant mice with defects in activity-dependent barrel development, such as *Lmo4* and *mGluR5* cortex-specific knockouts (Ballester-Rosado et al., 2010; Kashani et al., 2006). Lmo4 was of interest, because its expression was downregulated in *Lhx2* cKO S1 (Figure 3A) and it can potentially interact with Lhx2 through the LIM domain (Rétaux and Bachy, 2002). However, qRT-PCR analysis did not detect changes in the expression

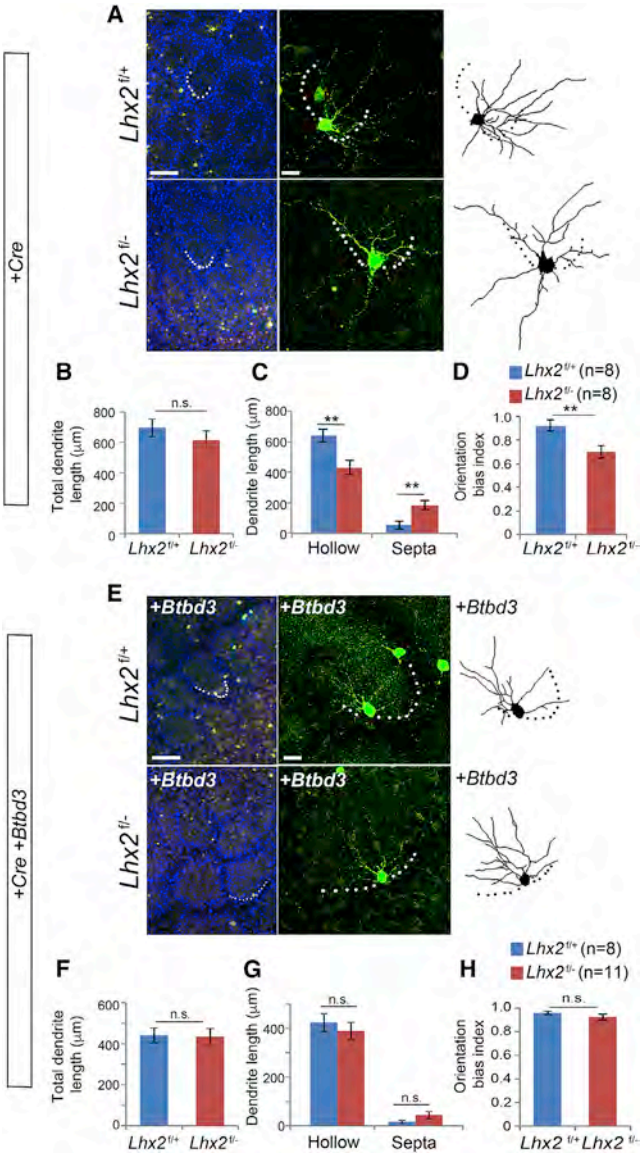

Figure 4. Lhx2 Regulates Dendritic Asymmetry of L4 Neurons via Btbd3

(A) CAG-Cre, CAG-mCherry, and the US-LNL-GFP reporter construct were co-electroporated into *Lhx2*$^{f/+}$ and *Lhx2*$^{f/-}$ embryonic cortices at E14.5 to generate WT (in *Lhx2*$^{f/+}$ cortices) and mutant (in *Lhx2*$^{f/-}$ cortices) L4 neurons. Immunostaining for GFP on tangential sections of flattened cortices reveals the morphology of WT and mutant L4 spiny stellate neurons, whose cell bodies were located in the barrel wall (dotted line) in P7 *Lhx2*$^{f/+}$ and *Lhx2*$^{f/-}$ cortices. Trace of GFP-positive cell morphology is shown on the right.

(B) Total dendritic length was comparable in WT and mutant cells.

(C) WT cells were polarized, with almost all dendrites projecting toward the barrel hollow; *Lhx2* mutant cells showed significantly decreased hollow-projecting dendritic length and significantly increased septa-projecting dendritic length ($p < 0.01$, $n = 8$).

(D) Orientation bias index (OBI), the ratio of the hollow projecting dendritic length to total dendritic length, was close to 1 in WT cells and was significantly decreased in mutant cells ($p < 0.01$, $n = 8$).

(E) A DNA mixture (as described in A) plus US2-myc-Btbd3 were electroporated into *Lhx2*$^{f/+}$ and *Lhx2*$^{f/-}$ embryonic cortices at E14.5. The electroporated L4 neuronal morphology was visualized as in (A).

(F) Total dendritic length is comparable in WT and Lhx2 mutant cells.

(G) Both WT and mutant cells show strong polarity, with almost all dendrites projecting toward to the hollow.

(H) Orientation bias index (OBI) was close to 1 in both WT and mutant cells.

Scale bars, 100 μm for left panels and 20 μm for right panels in (A) and (E). See also Figure S4.

of *Lhx2*, *Adcy1*, *Btbd3*, or *EfnA5* in *Lmo4* cortical mutant (*Lmo4*$^{f/f}$:*Nex*-Cre) S1 (Figure S4C). Unaffected expression of *Btbd3* in *Lmo4* cortical mutant S1 was further confirmed by in situ hybridization (Figure S4D). We also found unaffected *Btbd3* expression in *mGluR5* cortical mutant (*mGluR5*$^{f/f}$:*Nex*-Cre) S1 (Figure S4E). The maintained *Btbd3* expression in these mutants indicates that Lhx2 transcriptional regulation of *Btbd3* is independent of the function of Lmo4 or mGluR5, and it further suggests that the *Lhx2-Btbd3* genetic pathway is likely to function prior to the activity-dependent events of barrel development.

DISCUSSION

Due to its unique cytoarchitecture, the barrel cortex is widely used as a system to delineate the basics of circuit formation. Signaling pathways transmitting neuronal activities from TCA to L4 neurons promote TCA arborization in L4, L4 neuron aggregation to form barrel walls, and the development of L4 neuronal dendrites toward the barrel hollow (Li and Crair, 2011). Here, we uncover a mechanism whereby the transcription factor Lhx2, whose function was previously shown to be activity independent (Kashani et al., 2006), regulates the initiation of barrel cortex formation. In *Lhx2* cKO mice, we did not detect defects in the initial specification of L4 neurons or the initial VP TCAs entering the cortical plate. However, L4 neurons and TCAs did not develop further when *Lhx2* was selectively deleted in postmitotic cortical neurons, leading to a failure of barrel formation. This is likely due to the altered expression of several activity-regulated genes involved in regulating barrel formation in cKO mice. Thus, our findings place Lhx2 at the top of a genetic hierarchy for barrel development.

In this study, we provide evidence that Lhx2 regulates the development of L4 neuron dendritic asymmetry by directly inducing *Btbd3* expression in S1 L4. Knocking down *Btbd3* expression leads to a failure of L4 neurons to develop dendritic asymmetry (Matsui et al., 2013), similar to what we observed when deleting Lhx2. Intriguingly, *Btbd3* expression in S1 was downregulated in *Lhx2* cKO mice, similar to when VP TCA inputs were eliminated (Pouchelon et al., 2014). However, its expression remained in the S1 in cortex-specific knockouts of *NR1*, *mGluR5*, or *Lmo4* (Matsui et al., 2013; Figure S4), despite their defects in barrel formation (Ballester-Rosado et al., 2010; Kashani et al., 2006). As NR1, mGluR5, and Lmo4 were shown to mediate activity-dependent barrel development, based on our findings, we propose that Lhx2 functions in L4 neurons prior to activity-regulated events. Further, by inducing the expression of *Btbd3* and other activity-regulated genes, Lhx2 provides L4 neuronal competency to respond to TCA activities.

Further, our findings suggest that Lhx2 in postsynaptic L4 neurons is required for presynaptic TCAs to arborize in the barrel

hollow. The downregulation of *EphrinA5* and *Adcy1* in cKO S1 could possibly lead to TCA development defects, as EphrinA5 was proposed to induce TCA axonal arborization in S1 (Uziel et al., 2008) and *Adcy1* mutation reportedly led to changes in thalamocortical synaptic activity and TCA projection patterns (Abdel-Majid et al., 1998; Lu et al., 2003; Welker et al., 1996). Nevertheless, we found defects in patterning of barrel rows within cKO S1. It is likely that in L4 neurons, Lhx2 regulates the expression of key factors involved in patterning barrel cortex. In additional to its function in postmitotic neurons, Lhx2 is likely to play additional roles in cortical progenitors to regulate TCA development, as a previous study reported that the deletion of *Lhx2* in cortical progenitors via *Emx1*-Cre leads to an almost complete loss of TCAs in the cortex (Shetty et al., 2013). The fact that *Lhx2* deletion in cortical progenitors altered the timing of neurogenesis and led to a significantly decreased number of superficial layer neurons (Chou and O'Leary, 2013; Hsu et al., 2015) could contribute to the loss of TCAs in the cortex.

In conclusion, our study contributes to the understanding of the initial steps of barrel cortex circuit formation taken by L4 neurons to perceive TCA inputs. Lhx2 serves as a key regulator for the L4 neurons to form cellular barrels, develop dendritic asymmetry, and further induce TCA arborization.

EXPERIMENTAL PROCEDURES

Detailed experimental materials and methods and the different mouse lines used in this study, along with their sources, are described in Supplemental Experimental Procedures. All experiments were conducted in accordance with guidelines of the Academia Sinica Institutional Animal Care and Use Committee.

Immunohistochemistry, Immunostaining, and In Situ Hybridization

CO staining, immunostaining, and in situ hybridization using digoxigenin (DIG)-labeled riboprobes were performed as described previously (Chou et al., 2009; Zembrzycki et al., 2013).

Whisker Trimming and Enriched Environment Stimulation

Mice were anesthetized with Avertin (1.6 mg/mL, intraperitoneally [i.p.], 200 μL/10g body weight [b.w.]), and vibrissae on one side of the whisker pad were cut to fur level (<1 mm), except for C2. 1 day after recovery, mice were sacrificed after explored in enriched environment for 1 hr. The c-Fos distribution was measured by values of integrated density for the intensity of the fluorescence signals.

Chromatin Immunoprecipitation Assay

ChIP assays were performed as described previously (Carey et al., 2009). Dissociated cells from P7 WT S1 were fixed in 1% formaldehyde and then resuspended in lysis buffer (50 mM Tris [pH 8.0], 10 mM EDTA, 1% SDS, and 1× protease inhibitor). Chromatin was sonicated to an average size of 150–500 bp. 2μg antibodies (goat anti-Lhx2 antibody sc-19344 [Santa Cruz Biotechnology] or normal goat immunoglobulin G [IgG]) were used for immunoprecipitation. See Supplemental Experimental Procedures for primer sequences.

In Utero Electroporation

A DNA mixture containing US2-LNL (*loxP*-neomycin-Stop-*loxP*)-GFP (1.0 μg/μL), CAG-mCherry (0.2 μg/μL), and CAG-Cre (0.5 μg/μL) with or without US2-myc-Btbd3 (0.2 μg/μL) was electroporated into mouse dorsal telencephalon at E14.5 with paddle-type electrodes (CUY21 Electroporator) in a series of five square-wave current pulses (35 V, 100 ms × 5). Electroporated brains were collected at P7 for further analyses.

Statistical Analysis

Statistical analysis was performed using GraphPad Prism 5 software. Student's t test or ANOVA were used throughout the study. All data are expressed as mean ± SEM.

ACCESSION NUMBERS

The accession number for the microarray data reported in this paper is NCBI GEO: GSE92372.

SUPPLEMENTAL INFORMATION

Supplemental Information includes Supplemental Experimental Procedures, four figures, and two tables and can be found with this article online at http://dx.doi.org/10.1016/j.celrep.2017.01.001.

AUTHOR CONTRIBUTIONS

C.-F.W. and S.-J.C. designed the research and C.-F.W., H.-W.H., Z.-H.C., M.-H.W., W.-J.C., C.G.B., M.N., B.C.S., and S.-J.C. performed the research and analyzed data. S.-J.C. wrote the paper.

ACKNOWLEDGMENTS

We thank Dr. Dennis O'Leary for providing *Lhx2* floxed mice, Dr. Klaus-Armin Nave for *Nex*-Cre, Drs. Sam Pfaff and Soo-Kyung Lee for *Lmo4* floxed mice, and Dr. Hui-Chen Lu for *mGluR5* mutant brain tissues. We also thank Drs. Hwai-Jong Cheng and Hui-Chen Lu for critical reading and valuable comments and members of the Chou laboratory for their input and technical assistance. This work was supported by the Taiwan Ministry of Science and Technology (grants 104-2321-B-001-062 and 105-2321-B-001-042) (S.-J.C.) and the Institute of Cellular and Organismic Biology, Academia Sinica. M.N. is supported by the Ramón Areces Foundation, the Spanish Ministerio de Economía y Competetividad (MINECO; grants SAF2014-52119-R and BFU2014-55738-REDT). C.G.B. is supported by the Spanish Ministerio de Ciencia e Innovación (MICINN; fellowship FPI-BES-2012-056011).

Received: August 22, 2016
Revised: December 3, 2016
Accepted: December 29, 2016
Published: January 24, 2017

REFERENCES

Abdel-Majid, R.M., Leong, W.L., Schalkwyk, L.C., Smallman, D.S., Wong, S.T., Storm, D.R., Fine, A., Dobson, M.J., Guernsey, D.L., and Neumann, P.E. (1998). Loss of adenylyl cyclase I activity disrupts patterning of mouse somatosensory cortex. Nat. Genet. *19*, 289–291.

Ballester-Rosado, C.J., Albright, M.J., Wu, C.S., Liao, C.C., Zhu, J., Xu, J., Lee, L.J., and Lu, H.C. (2010). mGluR5 in cortical excitatory neurons exerts both cell-autonomous and -nonautonomous influences on cortical somatosensory circuit formation. J. Neurosci. *30*, 16896–16909.

Bulchand, S., Subramanian, L., and Tole, S. (2003). Dynamic spatiotemporal expression of LIM genes and cofactors in the embryonic and postnatal cerebral cortex. Dev. Dyn. *226*, 460–469.

Carey, M.F., Peterson, C.L., and Smale, S.T. (2009). Chromatin immunoprecipitation (ChIP). Cold Spring Harb. Protoc. *2009*, pdb prot5279.

Chen, T.C., Cheng, Y.Y., Sun, W.Z., and Shyu, B.C. (2008). Differential regulation of morphine antinociceptive effects by endogenous enkephalinergic system in the forebrain of mice. Mol. Pain *4*, 41.

Chou, S.J., and O'Leary, D.D. (2013). Role for Lhx2 in corticogenesis through regulation of progenitor differentiation. Mol. Cell. Neurosci. *56*, 1–9.

Chou, S.J., Perez-Garcia, C.G., Kroll, T.T., and O'Leary, D.D. (2009). Lhx2 specifies regional fate in Emx1 lineage of telencephalic progenitors generating cerebral cortex. Nat. Neurosci. *12*, 1381–1389.

Ding, Y.Q., Yin, J., Xu, H.M., Jacquin, M.F., and Chen, Z.F. (2003). Formation of whisker-related principal sensory nucleus-based lemniscal pathway requires a paired homeodomain transcription factor, Drg11. J. Neurosci. *23*, 7246–7254.

Erzurumlu, R.S., and Gaspar, P. (2012). Development and critical period plasticity of the barrel cortex. Eur. J. Neurosci. *35*, 1540–1553.

Erzurumlu, R.S., and Kind, P.C. (2001). Neural activity: sculptor of 'barrels' in the neocortex. Trends Neurosci. *24*, 589–595.

Goebbels, S., Bormuth, I., Bode, U., Hermanson, O., Schwab, M.H., and Nave, K.A. (2006). Genetic targeting of principal neurons in neocortex and hippocampus of NEX-Cre mice. Genesis *44*, 611–621.

Hou, P.S., Chuang, C.Y., Kao, C.F., Chou, S.J., Stone, L., Ho, H.N., Chien, C.L., and Kuo, H.C. (2013). LHX2 regulates the neural differentiation of human embryonic stem cells via transcriptional modulation of PAX6 and CER1. Nucleic Acids Res. *41*, 7753–7770.

Hsu, L.C., Nam, S., Cui, Y., Chang, C.P., Wang, C.F., Kuo, H.C., Touboul, J.D., and Chou, S.J. (2015). Lhx2 regulates the timing of β-catenin-dependent cortical neurogenesis. Proc. Natl. Acad. Sci. USA *112*, 12199–12204.

Ince-Dunn, G., Hall, B.J., Hu, S.C., Ripley, B., Huganir, R.L., Olson, J.M., Tapscott, S.J., and Ghosh, A. (2006). Regulation of thalamocortical patterning and synaptic maturation by NeuroD2. Neuron *49*, 683–695.

Jabaudon, D., Shnider, S.J., Tischfield, D.J., Galazo, M.J., and Macklis, J.D. (2012). RORβ induces barrel-like neuronal clusters in the developing neocortex. Cereb. Cortex *22*, 996–1006.

Kashani, A.H., Qiu, Z., Jurata, L., Lee, S.K., Pfaff, S., Goebbels, S., Nave, K.A., and Ghosh, A. (2006). Calcium activation of the LMO4 transcription complex and its role in the patterning of thalamocortical connections. J. Neurosci. *26*, 8398–8408.

Li, H., and Crair, M.C. (2011). How do barrels form in somatosensory cortex? Ann. N Y Acad. Sci. *1225*, 119–129.

Lu, H.C., She, W.C., Plas, D.T., Neumann, P.E., Janz, R., and Crair, M.C. (2003). Adenylyl cyclase I regulates AMPA receptor trafficking during mouse cortical 'barrel' map development. Nat. Neurosci. *6*, 939–947.

Matsui, A., Tran, M., Yoshida, A.C., Kikuchi, S.S., U, M., Ogawa, M., and Shimogori, T. (2013). BTBD3 controls dendrite orientation toward active axons in mammalian neocortex. Science *342*, 1114–1118.

Mi, H., Muruganujan, A., Casagrande, J.T., and Thomas, P.D. (2013). Large-scale gene function analysis with the PANTHER classification system. Nat. Protoc. *8*, 1551–1566.

Nakagawa, Y., Johnson, J.E., and O'Leary, D.D. (1999). Graded and areal expression patterns of regulatory genes and cadherins in embryonic neocortex independent of thalamocortical input. J. Neurosci. *19*, 10877–10885.

Petersen, C.C. (2007). The functional organization of the barrel cortex. Neuron *56*, 339–355.

Pouchelon, G., Gambino, F., Bellone, C., Telley, L., Vitali, I., Lüscher, C., Holtmaat, A., and Jabaudon, D. (2014). Modality-specific thalamocortical inputs instruct the identity of postsynaptic L4 neurons. Nature *511*, 471–474.

Rebsam, A., Seif, I., and Gaspar, P. (2005). Dissociating barrel development and lesion-induced plasticity in the mouse somatosensory cortex. J. Neurosci. *25*, 706–710.

Rétaux, S., and Bachy, I. (2002). A short history of LIM domains (1993-2002): from protein interaction to degradation. Mol. Neurobiol. *26*, 269–281.

Roberson, M.S., Schoderbek, W.E., Tremml, G., and Maurer, R.A. (1994). Activation of the glycoprotein hormone alpha-subunit promoter by a LIM-homeodomain transcription factor. Mol. Cell. Biol. *14*, 2985–2993.

Rodríguez-Tornos, F.M., San Aniceto, I., Cubelos, B., and Nieto, M. (2013). Enrichment of conserved synaptic activity-responsive element in neuronal genes predicts a coordinated response of MEF2, CREB and SRF. PLoS ONE *8*, e53848.

Shetty, A.S., Godbole, G., Maheshwari, U., Padmanabhan, H., Chaudhary, R., Muralidharan, B., Hou, P.S., Monuki, E.S., Kuo, H.C., Rema, V., and Tole, S. (2013). Lhx2 regulates a cortex-specific mechanism for barrel formation. Proc. Natl. Acad. Sci. USA *110*, E4913–E4921.

Shirasaki, R., and Pfaff, S.L. (2002). Transcriptional codes and the control of neuronal identity. Annu. Rev. Neurosci. *25*, 251–281.

Uziel, D., Mühlfriedel, S., and Bolz, J. (2008). Ephrin-A5 promotes the formation of terminal thalamocortical arbors. Neuroreport *19*, 877–881.

Vitali, I., and Jabaudon, D. (2014). Synaptic biology of barrel cortex circuit assembly. Semin. Cell Dev. Biol. *35*, 156–164.

Welker, E., Armstrong-James, M., Bronchti, G., Ourednik, W., Gheorghita-Baechler, F., Dubois, R., Guernsey, D.L., Van der Loos, H., and Neumann, P.E. (1996). Altered sensory processing in the somatosensory cortex of the mouse mutant barrelless. Science *271*, 1864–1867.

Wu, C.S., Ballester Rosado, C.J., and Lu, H.C. (2011). What can we get from 'barrels': the rodent barrel cortex as a model for studying the establishment of neural circuits. Eur. J. Neurosci. *34*, 1663–1676.

Yang, J.W., Shih, H.C., and Shyu, B.C. (2006). Intracortical circuits in rat anterior cingulate cortex are activated by nociceptive inputs mediated by medial thalamus. J. Neurophysiol. *96*, 3409–3422.

Zembrzycki, A., Chou, S.J., Ashery-Padan, R., Stoykova, A., and O'Leary, D.D. (2013). Sensory cortex limits cortical maps and drives top-down plasticity in thalamocortical circuits. Nat Neurosci. *16*, 1060–1067.

Zembrzycki, A., Perez-Garcia, C.G., Wang, C.F., Chou, S.J., and O'Leary, D.D. (2015). Postmitotic regulation of sensory area patterning in the mammalian neocortex by Lhx2. Proc. Natl. Acad. Sci. USA *112*, 6736–6741.